Characterization of electric load with Information Theory quantifiers

CrossMark

Andre L.L. Aquino [a,*], Heitor S. Ramos [a], Alejandro C. Frery [a],
Leonardo P. Viana [a], Tamer S.G. Cavalcante [b], Osvaldo A. Rosso [c,d,e]

[a] LaCCAN/CPMAT – Instituto de Computação, Universidade Federal de Alagoas (UFAL), BR 104 Norte km 97, 57072-970 Maceió, Alagoas, Brazil
[b] Centro de Informática, Universidade Federal de Pernambuco (UFPE), Av. Professor Moraes Rego 1235, 50670–901 Recife, Pernambuco, Brazil
[c] Instituto de Física, Universidade Federal de Alagoas (UFAL), BR 104 Norte km 97, 57072-970 Maceió, Alagoas, Brazil
[d] Instituto Tecnológico de Buenos Aires (ITBA), CONICET, C1106ACD, Av. Eduardo Madero 399, Ciudad Autónoma de Buenos Aires, Argentina
[e] Complex Systems Group, Facultad de Ingeniería y Ciencias Aplicadas, Universidad de los Andes, Av. Mons. Álvaro del Portillo 12.455, Las Condes, Santiago, Chile

HIGHLIGHTS

- We use Information Theory for the characterization of electric load.
- With our characterization was identified different regimes and behaviors in the electric load.
- We observe that types of appliances have characteristic footprints that form clusters in the CCE plane.

ARTICLE INFO

ABSTRACT

This paper presents a study of the electric load behavior based on the Causality Complexity–Entropy Plane. We use a public data set, namely REDD, which contains detailed power usage information from several domestic appliances. In our characterization, we use the available power data of the circuit/devices of all houses. The Bandt–Pompe methodology combined with the Causality Complexity–Entropy Plane was used to identify and characterize regimes and behaviors over these data. The results showed that this characterization provides a useful insight into the underlying dynamics that govern the electric load.

© 2016 Elsevier B.V. All rights reserved.

1. Introduction

Traditionally, power grids are used to carry power from a few central generators to a large number of users or customers. In contrast, Smart Grids use two-way flows of electricity and information to create an automated and distributed advanced energy delivery network [1]. Smart Grids enable the development of new applications related to advanced information metering, monitoring, and management, for instance, Non-Intrusive Load Monitoring (NILM) [2,3].

---

* Corresponding author.
  E-mail address: alla.lins@gmail.com (A.L.L. Aquino).

Zoha et al. [2] state that NILM requires disaggregating electrical loads by examining only appliance specific power consumption signatures within the aggregated load data. The data is acquired from the main electrical panel outside the building or the residence, hence it is considered to be non-intrusive as the method does not require any equipment installation inside the customer's property. The goal is to breakdown the whole-house building data into its major constituents.

A key aspect to explore in NILM applications is the adequate characterization of electrical energy consumption of domestic appliances. To tackle this issue we present a characterization of the behavior of electrical devices by using quantifiers stemming from Information Theory. The characterization is performed in two stages. Firstly, the original time series of the electrical consumption is transformed into a histogram with a nonparametric transformation that retains time causal information: the Bandt–Pompe methodology [4]. Secondly, this histogram is mapped onto the Causality Complexity–Entropy Plane (CCEP) [5], and its location is shown to serve as a characterization of a number of typical regimes. This plane is a compact manifold spanning values of the normalized Shannon entropy $\mathcal{H}$ and the statistical complexity $\mathcal{C}$.

According to the findings obtained by Rosso et al. [5], chaotic maps have intermediate $\mathcal{H}$ values, while $\mathcal{C}$ stays close to the maximum possible complexity value [6]. For regular processes, entropy and complexity have small values, close to zero. Finally, totally uncorrelated stochastic processes are located close to the (1, 0) point. It has also been found that $1/f^k$ correlated stochastic processes with $1 \leq k \leq 3$ are characterized by intermediate permutation entropy and intermediate statistical complexity values [5]. Additionally, they found that fractional Gaussian noise (fGn) fingerprints lie in the same region than $0 \leq k < 1$ noise. Fractional Brownian motion (fBm) sweeps the region equivalent to $1 \leq k \leq 3$ noise, with two important particular cases: antipersistent fBm ($1 \leq k < 2$), and persistent fBm ($2 \leq k \leq 3$). Note that these processes lie in different positions in the CCEP and, thus, can be characterized by two watersheds: those below and above what looks like a division line. Our assumption is that using a similar methodology we would be able to characterize the dynamic behavior of appliances.

We conduct an exploratory study to test our methodology with time series from the REDD (Reference Energy Disaggregation Data Set) data set, which describes the power usage information of several domestic appliances [7]. The characterization herein performed uses the available power data of circuits/devices collected from five houses. We analyze devices that can be classified into two different modes of operation: (i) devices that are continuously switched on, such as refrigerators, and (ii) devices that can be switched on or off due to human intervention or any kind of automation, such as oven, lamp and washing machines. Although the information about the intervals that devices are switched on or off can be used to characterize the device, in this work we are mostly interested in the dynamics of the power consumption behavior only when a device is switched on. Thus, we pre-processed the data to rule out all zero readings to capture this situation.

This work is organized as following: Section 2 presents the related work. Section 3 explains the Information Theory quantifiers. Section 4 discusses the energy information data set. Section 5 presents the obtained results. Finally, Section 6 concludes the manuscript.

2. Related work

The characterization of electrical energy consumption of domestic appliances in NILM applications is largely underexplored. Among the problems tackled in the literature, Refs. [8–10] discuss techniques for event detection. Rather than focusing on such problem, other approaches treat the issue of energy disaggregation, i.e., they estimate the energy consumed by devices operating in different ranges of power consumption [11–13]. These works are based on finding correspondences between known and observed patterns.

A number of tools have been used to deal with the NILM problem, event detection or complete disaggregation, among them: hidden Markov models [7,12]; fuzzy systems [13,14]; k-nearest neighbors [15]; evolutionary algorithms [16,17]; k-means [11]; and support vector machines [18]. These works analyze the data for specific applications in mind, whereas in this work we propose an application-free approach that uses a tool based on information-theoretic descriptors that have not been employed previously for this problem.

Several data sets are available, among them: Reference Energy Disaggregation Data Set (REDD) [7]; Building-Level fUlly-labeled data set for Electricity Disaggregation (BLUED) [19]; UK recording Domestic Appliance-Level Electricity (UK-DALE) [20]; Smart* [20]; and the Berkeley campus energy portal (Openbms) [21]. Our testbed is the REDD data base because its low sampling frequency turns the characterization problem more challenging and realistic. This kind of data is the one produced by off-shelf equipment and, thus, contributes for reproducibility of the study both experimentally and theoretically.

Finally, several works investigate the usage of information theory quantifiers to characterize the dynamics underlying time series, for instance, the effects of streamflow dynamics [22], unsupervised edge map scoring [23], and stochastic resonance in a bistable system [24]. Additionally, theoretical advances in statistical complexity measure are discussed in Refs. [25–27].

3. Time series and information theory quantifiers

Bandt and Pompe [4] introduced a method to associate a probability distribution from a time series taking into account the time causality of the process. Given a time series $\boldsymbol{X}(t) = \{x_t : t = 1, \ldots, M\}$, an embedding dimension $D \geq 2$ ($D \in \mathbb{N}$),

and an embedding delay time $\tau \in \mathbb{N}$, we compute the ordinal patterns of order D (pattern length) generated by

$$(s) \mapsto \left(x_{s-(D-1)\tau}, x_{s-(D-2)\tau}, \ldots, x_{s-\tau}, x_s\right), \tag{1}$$

i.e., for each instant s, we assign a D dimensional vector that results from the evaluation of the series at times $s - (D - 1)\tau$, $\ldots, s - \tau, s$. The larger the D, the more information about the past is incorporated into the vectors. By the ordinal pattern of order D related to the time instant s we mean the permutation $\pi = \{r_0, r_1, \ldots, r_{D-1}\}$ of $\{0, 1, \ldots, D - 1\}$ defined by

$$x_{s-r_{D-1}\tau} \le x_{s-r_{D-2}\tau} \le \cdots \le x_{s-r_1\tau} \le x_{s-r_0\tau}. \tag{2}$$

In this way, the vector defined by Eq. (1) is converted into a unique symbol π. In order to get a unique result we set $r_i < r_{i-1}$ if $x_{s-r_i} = x_{s-r_{i-1}}$. Equal values have probability zero if $\boldsymbol{X}(t)$ follows a continuous distribution marginally.

Thus, for all the $D!$ possible permutations π of order D, their associated relative frequencies can be computed by the number of times this particular order sequence is found in the time series divided by the total number of sequences. The histogram $P \equiv \{p(\pi)\}$ is defined by

$$p(\pi) = \frac{\#\{s \text{ of type } \pi : s \le M - (D - 1)\tau\}}{M - (D - 1)\tau}, \tag{3}$$

where # is the cardinality of the set.

This histogram approximates a probability function P (Bandt–Pompe PDF), and is linked to the sequences of ranks resulting from the comparison of consecutive ($\tau = 1$) or non-consecutive ($\tau > 1$) points, allowing for the empirical reconstruction of the underlying phase space, even in the presence of weak (observational and dynamic) noise [4]. The embedding delay τ is the time separation between series data, and different values of τ, which corresponds to multiples of the sampling time of the signal under analysis, could provide additional information. Zunino et al. [28] showed that this parameter is strongly related, when it is relevant, to the intrinsic time scales of the system under analysis.

The embedding dimension D plays an important role in the evaluation of probability distribution P because D determines the number of accessible states $D!$ and also conditions the minimum acceptable length $M \gg D!$ of the time series that one needs in order to work with reliable statistics [5]. Furthermore, the ordinal patterns associated with P are invariant with respect to nonlinear monotonic transformations. Accordingly, nonlinear drifts or scaling artificially introduced by a measurement device will not modify the estimation of quantifiers, a nice property if one deals with experimental data [29]. These advantages make the Bandt–Pompe methodology more convenient than conventional methods based on range partitioning.

In this work we evaluate the normalized Shannon entropy and the Statistical Complexity of the histogram P obtained with the Bandt–Pompe methodology over time series of electric load. Since this methodology consists of counting sequences of symbols, the former quantifier is called *permutation Normalized Shannon Entropy* and the latter *permutation Statistical Complexity*.

Let $\varXi$ be a discrete random variable with $M < \infty$ possible values $\varOmega = \{\xi_i : i = 1, \ldots, M\}$ and whose distribution is characterized by the probability function $P = \{p_j \ge 0 : j = 1, \ldots, N\}$ and $\sum_{j=0}^{N} p_j = 1$. The Shannon logarithmic information measure [30] is $\mathcal{S}[P] = -\sum_{j=1}^{N} p_j \ln p_j$, where, by convention, $0 \ln 0 = 0$. The Shannon Entropy is related to the information associated with the physical process described by P.

A reference distribution is the uniform over $\varOmega$, which is characterized by $p_j = N^{-1}$ for every $1 \le j \le N$. Denoting this distribution as P_e, it is immediate that $\mathcal{S}[P_e] = \ln N$. This is the maximum possible entropy of a discrete system, and describes the situation of less information about the process.

Lamberti et al. [31] introduced the Statistical complexity measure $\mathcal{C}_{JS}$ that is able to detect essential details of the underlying dynamics that gives rise to the observations. This measure is defined according to the functional product proposed by López-Ruiz et al. [32]:

$$\mathcal{C}_{JS}[P] = \mathcal{H}_S[P] \, \mathcal{Q}_{JS}[P, P_e], \tag{4}$$

where

$$\mathcal{H}_S[P] = \mathcal{S}[P] / \mathcal{S}^{\max} \tag{5}$$

is the normalized Shannon Entropy $\mathcal{H}_S \in [0, 1]$ with $\mathcal{S}^{\max} = \mathcal{S}[P_e]$, and the disequilibrium $\mathcal{Q}_{JS}$ is defined in terms of the extensive (in the thermodynamical sense) Jensen–Shannon divergence, namely,

$$
\begin{aligned}
\mathcal{Q}_{JS}[P, P_e] &= Q_0 \, \mathcal{J}_S[P, P_e] \\
&= Q_0 \left\{ \mathcal{S}\left[\frac{P + P_e}{2}\right] - \frac{\mathcal{S}[P] + \mathcal{S}[P_e]}{2} \right\};
\end{aligned} \tag{6}
$$

here Q_0 is a normalization constant equal to the inverse of the maximum possible value of $\mathcal{J}_S[P, P_e]$ so that $\mathcal{Q}_{JS} \in [0, 1]$. Q_0 is obtained when one of the probabilities of P is equal to one and the remaining are equal to zero.

The temporal evolution of $\mathcal{H}_S$ and $\mathcal{C}_{JS}$ can be analyzed using a two-dimensional diagram, called Causality Complexity–Entropy Plane (CCEP). The CCEP is obtained by plotting $\mathcal{C}_{JS}$ (vertical axis) versus $\mathcal{H}_S$ (horizontal axis) [5]. For

a given value of $\mathcal{H}_S$, the range of possible $\mathcal{C}_{JS}$ values, in this plane, varies between $\mathcal{C}_{JS}^{min}$ and $\mathcal{C}_{JS}^{max}$ [6]. The term "causality" reminds the fact that temporal correlations between successive samples are taken into account through $P = \{ p(\pi) \}$, the PDF computed with the Bandt–Pompe methodology used to evaluate both Information Theory quantifiers $\mathcal{H}_S$ and $\mathcal{C}_{JS}$.

This diagnostic tool was shown to be particularly efficient at distinguishing between the deterministic chaotic and stochastic nature of time series, since the permutation quantifiers have distinctive behaviors for different types of dynamics. Rosso et al. [5] showed that chaotic maps have intermediate $\mathcal{H}_S$ values, while $\mathcal{C}_{JS}$ reaches larger values, close to those of the limit $\mathcal{C}_{JS}^{max}$. For regular processes, both quantifiers have small values, close to zero. Finally, totally uncorrelated stochastic processes are close to $\mathcal{H}_S \approx 1$ and $\mathcal{C}_{JS} \approx 0$. Correlated stochastic processes with f^{-k} power spectrum ($0 < k \leq 3$) are characterized by intermediate permutation entropy and intermediate statistical complexity values between $\mathcal{C}_{JS}^{min}$ and $\mathcal{C}_{JS}^{max}$. Similar planar localization was also found for fractional Brownian motion (fBm) and fractional Gaussian noise (fGn) dynamics [5]. For a review of Bandt and Pompes methodology and its applications to physics, biomedical and econophysics signals, see Refs. [33–38].

4. Power data characterization

The REDD data set contains information about the energy consumption of several real houses organized into logs with the total consumption of a household, or logs of individual devices. The whole home electricity signal was recorded for each house (current was monitored on both phases and voltage was monitored on one phase) at a high frequency (15 kHz). Data was collected from up to 24 individual circuits in the house, each labeled with its category of appliance or appliances, recorded at 0.5 Hz; and up to 20 plug-level monitors in the home, recorded at 1 Hz, with a focus on logging electronics devices where multiple devices are grouped to a single circuit. Data were collected on ten houses, over 119 days, 268 unique monitors, and comprise more than 1 TiB of raw data.

We used the available power data of all devices and individual circuits of five houses. Some of the devices and individuals circuits used are: furnace, refrigerator, air conditioning, dishwasher, lighting, kitchen outlets, and general use outlets. Part of the original time series of furnace and refrigerator is illustrated in Fig. 1: only the first 100000 samples are shown, whereas the original time series have 404107 and 318759 observations, respectively. Observe that the furnace shown in Fig. 1(a) corresponds to a device that is not continuously switched on as many consecutive zero readings are observed and the refrigerator data shown in Fig. 1(b) corresponds to a device that is continuously on as no long periods of zero readings are observed. As the Bandt–Pompe PDF can be heavily biased due to the presence of several zero readings such as shown in Fig. 1(a), we opt to pre-process the data to rule out these readings. Hence, we focus on the dynamical behavior of the load when its circuitry is energized.

Initially we removed all values less than 50 W; zeros occur when the device is off. Small readings occur when devices are in low-power mode (sleep) and only few circuits are energized, for instance, a status led is on. Few clearly discrepant observations were also deleted. Such pre-processing was performed because we are interested in characterizing the main usage of each device or circuit.

Fig. 2 presents the time series associated to the furnace #1 (there are three furnaces in the data set) and to the refrigerator #2 (there are 5 refrigerators), after the signal pre-processing described in the previous paragraph. In this illustration we use only the first 2000 samples, but the original ones have 6432 (furnace) and 141550 (refrigerator) respectively. As observed, the furnace (Fig. 2(a)) and the refrigerator (Fig. 2(b)) present near periodic behaviors with different period and power waveform. The rationale behind this periodic behavior is because these devices are controlled by a thermostat and, for instance, the refrigerator's compressor can be switched on and off to control the temperature. A similar behavior is found in the furnace #2 data, but we can observe different dynamics between these two different devices. This is what we are mostly interested to capture. In the sequel, we will see that these and other patterns are mapped into different points and regions of the CCEP.

5. Results and discussions

In our proposal, we associate a probability distribution function to time series with the Bandt–Pompe symbolization [4]. Bandt and Pompe suggest to use embedding dimensions between 3 and 7. We used $D = 4$, and the embedding delay time $\tau = 1$ with good results: the observed clusters have a nice interpretation. Larger length patterns do not lead to significantly different localizations and, due to the number of observations in the available time series, they introduce more variability.

The probability distribution functions of patterns from the aforementioned time series are shown in Fig. 3. For instance, the pattern 0123 counts the number of increasing power readings in four consecutive samples. Fig. 3(a) shows that the probability of this pattern is close to 7% in the furnace #1 data set.

Observing the histograms in Fig. 3, it is possible to identify differences among the analyzed devices. Specifically, Fig. 3(a) presents all patterns close to 5%. In the same way, but in a smaller proportion, Fig. 3(b) shows that some patterns (3201, 3210, and 2310) are less frequent than the majority. The behavior of each device or individual circuit can be further analyzed by computing $\mathcal{H}_S$ and $\mathcal{C}_{JS}$ for these distributions, as presented in Section 3.

In order to compare our power data with stochastic processes, we generated colored noises with f^{-k} ($k \geq 0$) power spectrum [5]. The sequences were of length $M = 10^6$, and we used the same pattern length ($D = 4$) and embedding
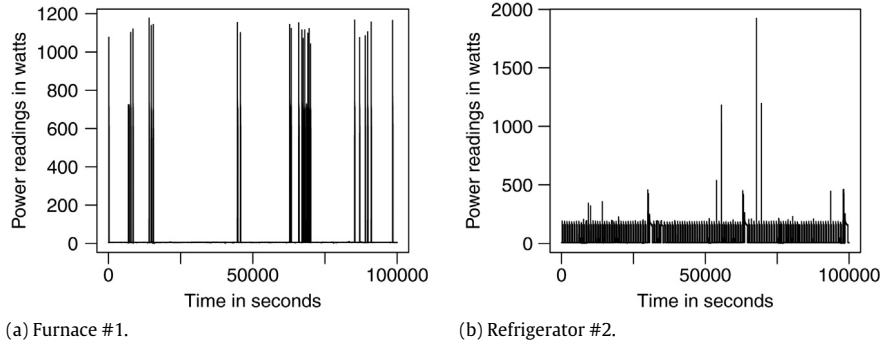
(a) Furnace #1.   (b) Refrigerator #2.

Fig. 1. Original energy consumption time series for furnace and refrigerator.

(a) Furnace #1.   (b) Refrigerator #2.
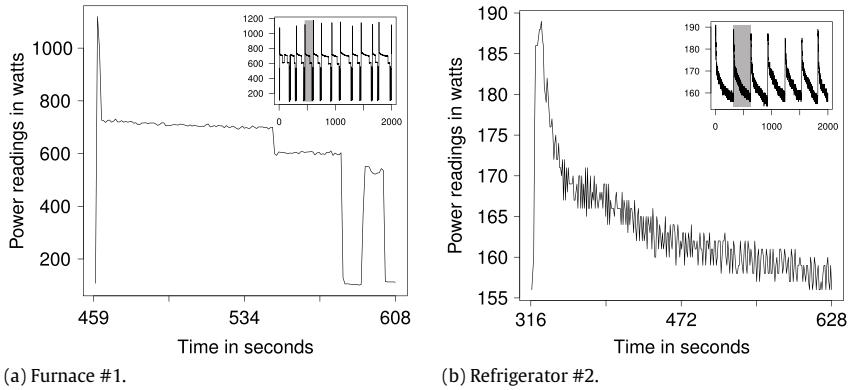
Fig. 2. After pre-processing energy consumption time series for furnace and refrigerator.
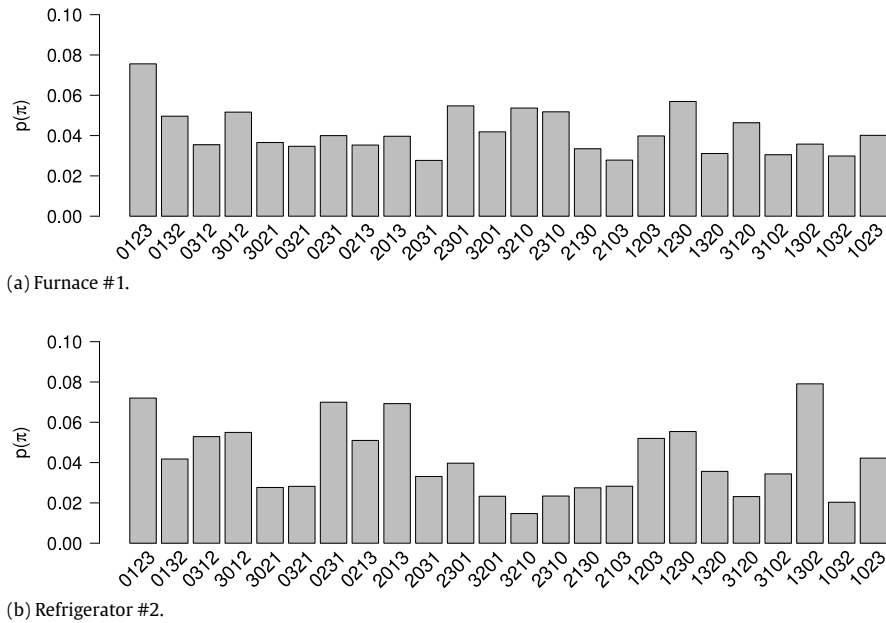

(a) Furnace #1.

(b) Refrigerator #2.

Fig. 3. Bandt–Pompe PDF, $D = 4$ and $\tau = 1$ for (pre-processing) energy consumption time series for furnace and refrigerator.

delay ($\tau = 1$) employed for the observed time series. These colored noises help us understand the randomness of dynamic systems, as they can be used as references in the Causality $\mathcal{H} \times \mathcal{C}$-plane. For instance, times series located close to the point where the process $k = 1$ is located are less correlated than those close to $k = 3$.
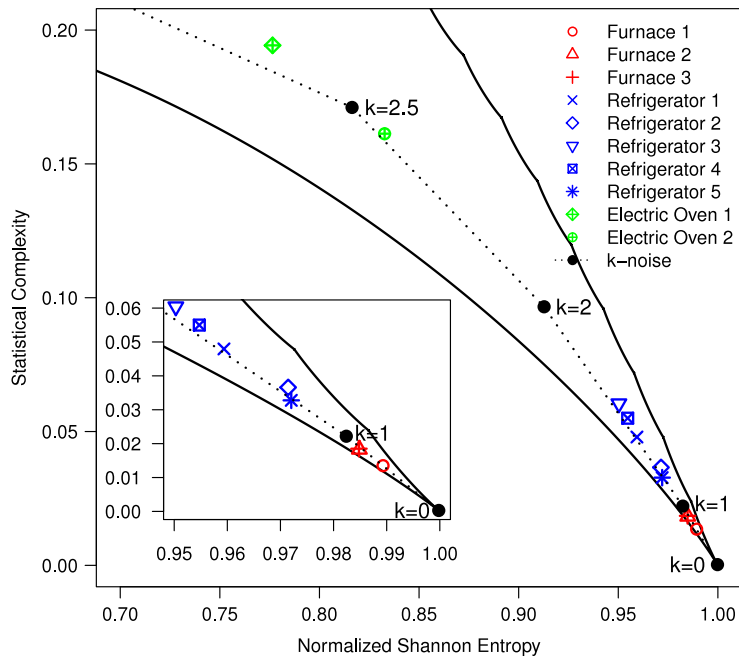
Fig. 4. CCEP ($D = 4$ and $\tau = 1$) with points from furnaces, refrigerators and electric ovens. Continues curves correspond to the $\mathcal{C}_{JS}^{min}$ and $\mathcal{C}_{JS}^{max}$ [6]. (For interpretation of the references to color in this figure legend, the reader is referred to the web version of this article.)

Fig. 4 shows the Causality Complexity–Entropy Plane for embedding dimensions $D = 4$ and time lag $\tau = 1$. The points from three devices categories (three furnaces, five refrigerators, and two electric ovens) are presented along with those from colored noise f^{-k} with $k = \{0, 1, 2, 2.5\}$. The dotted segments are used to guide the visualization. Solid lines represent the limits in the CCEP within which any possible dynamic system lies [6].

It is interesting to notice that, as shown in Fig. 4, the points in the CCEP form clusters according to their categories while, at the same time, they lie close to the segments that characterize f^{-k} noise. The furnaces (red points) are closest to pure randomness, i.e., to the $k = 0$ reference; they all lie in the region below $k = 1$, so these processes are the ones that exhibit less correlation. From the time series shown in Fig. 2, we observe that both, the furnace #1 and the refrigerator #2 present a noisy behavior, being the refrigerator #2 the one that presents more correlation. It is worth to mention that the value of the power reading is not considered in Bandt–Pompe methodology, only the up and down patterns are considered. Thus, we observe in Fig. 4 that the furnace #1 shows up in the CCEP close to the pink noise ($k = 1$), while the refrigerator #2 is between pink and brown noise ($k = 2$). Actually, all five refrigerators are characterized by points between pink and brown noises. The ovens lie at the other extreme, around the point that characterizes $k = 2.5$ noise (black noise), so with the highest observed correlation.

Additionally, we evaluate the signatures of washer–dryers and lamps circuits in the CCEP. Fig. 5 presents the signatures of all washer–dryers and lamps circuits in the CCEP. Washer–dryers form two groups: one between $0 < k < 1$ and other near $k = 2.5$. The REDD data set does not provide the specification of each device or circuit used. So, we hypothesize that there are different types of washer–dryers and user profiles in the data set.

The lamps circuits were analyzed as a whole, and not by individual elements. In the same manner, two groups of lamps circuits were observed. The first group is comprised of seven footprints, located in the regular region on the CCEP of intermediate values of $\mathcal{C}_{JS}$ and low values of $\mathcal{H}_S$ (Fig. 5). The second group consists of six signatures with behavior similar to colored noise ($1 < k < 3$). Again, our hypothesis is that there are different types of lamps and user profiles in the data set.

The aggregation of lamps in circuits precludes a finer analysis of the behavior of types of lamps as, for instance, incandescent, LEDs and fluorescent lamps have different footprints.

6. Conclusion and future work

This work presents a novel characterization of the electric load behavior. This characterization contributes for a better understanding of the underlying dynamics governing this process, and to improve the design of smart grid applications.

The proposal consists of counting small-length scale-invariant patterns in the time series: the Bandt–Pompe methodology. Two based Information Theory quantifiers are then extracted from the histogram of such features: the normalized permutation Shannon entropy $\mathcal{H}_S$ and the permutation statistical complexity $\mathcal{C}_{JS}$. This footprint is then plotted in the CCEP.

Types of appliances have characteristic footprints that form clusters in the CCEP. These clusters form around or close to reference points that correspond to well-known dynamical systems and types of noise. The output of classes of appliances
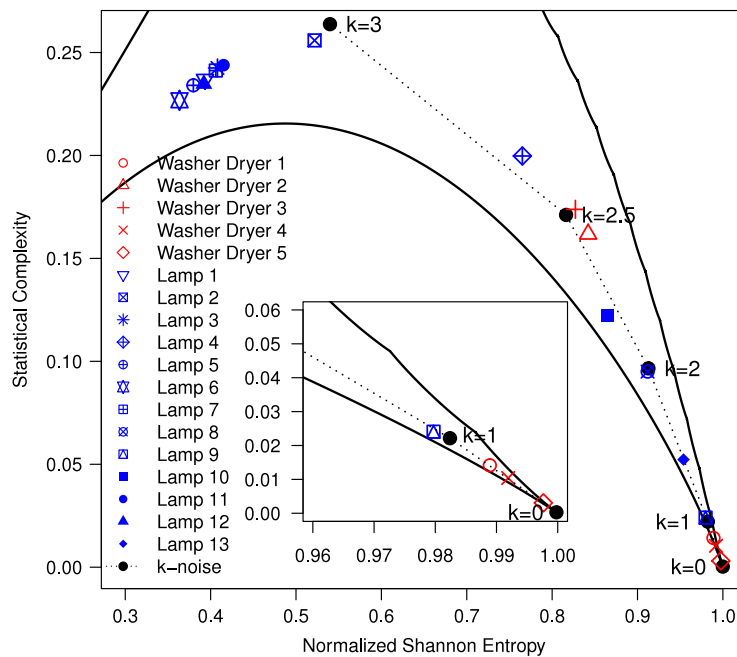
Fig. 5. CCEP ($D = 4$ and $\tau = 1$) with points from washer–dryers and lamps circuits. Continues curves correspond to the $\mathcal{C}_{JS}^{\min}$ and $\mathcal{C}_{JS}^{\max}$ [6].

can be, thus, associated to these objects and to their characteristic correlation lengths and memory. This is a qualitative characterization rather than a quantitative one, as we cannot affirm that the appliances themselves behave as f^{-k} noise.

These clusters are easily identifiable, as they induce simple rules for their separation. This opens promising venues for research, as the mapping of time series into points in the CCEP is model-free, is both computationally inexpensive and of low dimensionality. This contrasts with previous results on Energy Disaggregation, that required high-dimensional features that are computationally demanding to obtain [39–42].

Among the current proposals for Non-Intrusive Load Monitoring (NIML) [2,3,43] our proposed method presents a different approach through the characterization of the energy load dynamics properties. The Bandt–Pompe methodology proved to be effective in the identification of electric appliances behavior, thus opening further opportunities to both practical applications and theoretical challenges. We will apply the proposed characterization to other data sets, and this methodology will be used to perform both non-intrusive energy disaggregation and finer household identification.

Acknowledgments

References

[1] X. Fang, S. Misra, G. Xue, D. Yang, Smart grid - The new and improved power grid: A survey, Commun. Surv. Tutor. 14 (4) (2012) 944–980.
[2] A. Zoha, A. Gluhak, M.A. Imran, S. Rajasegarar, Non-intrusive load monitoring approaches for disaggregated energy sensing: A survey, Sensors 12 (12) (2012) 16838–16866.
[3] A.S. Bouhouras, A.N. Milioudis, D.P. Labridis, Development of distinct load signatures for higher efficiency of NILM algorithms, Electr. Power Syst. Res. 117 (1) (2014) 163–171.
[4] C. Bandt, B. Pompe, Permutation entropy: A natural complexity measure for time series, Phys. Rev. Lett. 88 (2002) 174102–174106.
[5] O.A. Rosso, H.A. Larrondo, M.T. Martín, A. Plastino, M.A. Fuentes, Distinguishing noise from chaos, Phys. Rev. Lett. 99 (15) (2007) 154102.
[6] M. Martín, A. Plastino, O.A. Rosso, Generalized statistical complexity measures: Geometrical and analytical properties, Physica A 369 (2) (2006) 439–462.
[7] J.Z. Kolter, M.J. Johnson, REDD: A public data set for energy disaggregation research, in: 1st KDD Workshop on Data Mining Applications in Sustainability (SustKDD), 2011.
[8] S.B. Leeb, S.R. Shaw, J. Kirtley, J.L. , Transient event detection in spectral envelope estimates for nonintrusive load monitoring, IEEE Trans. Power Deliv. 10 (3) (1995) 1200–1210.
[9] K.S. Barsim, R. Streubel, B. Yang, An approach for unsupervised non-intrusive load monitoring of residential appliances, in: 2nd Non-Intrusive Load Monitoring Workshop (NILM), 2014.
[10] K. Anderson, M. Berges, A. Ocneanu, D. Benitez, J. Moura, Event detection for non intrusive load monitoring, in: 38th Annual Conference on IEEE Industrial Electronics Society (IECON), 2012, pp. 3312–3317.
[11] K. Anderson, J.M.F. Moura, M. Berges, Unsupervised approximate power trace decomposition algorithm, in: 2nd Non-Intrusive Load Monitoring Workshop (NILM), 2014.

[12] O. Parson, S. Ghosh, M. Weal, A. Rogers, An unsupervised training method for non-intrusive appliance load monitoring, Artif. Intell. 217 (1) (2014) 1–19.
[13] Y.-H. Lin, M.-S. Tsai, C.-S. Chen, Applications of fuzzy classification with fuzzy c-means clustering and optimization strategies for load identification in NILM systems, in: IEEE International Conference on Fuzzy Systems (FUZZ-IEEE), 2011, pp. 859–866.
[14] Y.-H. Lin, M.-S. Tsai, Non-intrusive load monitoring by novel neuro-fuzzy classification considering uncertainties, IEEE Trans. Smart Grid 5 (5) (2014) 2376–2384.
[15] T.R. Camier, S. Giroux, B. Bouchard, A. Bouzouane, Designing a NIALM in smart homes for cognitive assistance, in: 4th International Conference on Ambient Systems, Networks and Technologies (ANT) and 3rd International Conference on Sustainable Energy Information Technology (SEIT), 2013, pp. 524–532.
[16] D. Egarter, A. Sobe, W. Elmenreich, Evolving non-intrusive load monitoring, in: 16th European Conference on Applications of Evolutionary Computation, 2013, pp. 182–191.
[17] H.-H. Chang, L.-S. Lin, N. Chen, W.-J. Lee, Particle-swarm-optimization-based nonintrusive demand monitoring and load identification in smart meters, IEEE Trans. Ind. Appl. 49 (5) (2013) 2229–2236.
[18] M. Figueiredo, A. de Almeida, B. Ribeiro, Home electrical signal disaggregation for non-intrusive load monitoring (NILM) systems, Neurocomputing 96 (1) (2012) 66–73. Adaptive and Natural Computing Algorithms.
[19] K. Anderson, A. Ocneanu, D. Benitez, D. Carlson, A. Rowe, M. Berges, BLUED: a fully labeled public dataset for Event-Based Non-Intrusive load monitoring research, in: 2nd KDD Workshop on Data Mining Applications in Sustainability (SustKDD), 2012.
[20] J. Kelly, W.J. Knottenbelt, The UK-DALE dataset, domestic appliance-level electricity demand and whole-house demand from five UK homes, Sci. Data 2 (1) (2015) 150007.
[21] Openbms, a Berkeley campus energy portal 2013. URL http://berkeley.openbms.org/.
[22] T. Stosic, L. Telesca, D.V. de Souza Ferreira, B. Stosic, Investigating anthropically induced effects in streamflow dynamics by using permutation entropy and statistical complexity analysis: A case study, J. Hydrol. 540 (2016) 1136–1145.
[23] J. Gimenez, J. Martinez, A.G. Flesia, Unsupervised edge map scoring: A statistical complexity approach, Comput. Vis. Image Underst. 122 (2014) 131–142.
[24] L. Rudnicki, I.V. Toranzo, P. Sánchez-Moreno, J.S. Dehesa, Monotone measures of statistical complexity, Phys. Rev. A 380 (2016) 377–380.
[25] M. He, W. Xu, Z. Sun, L. Du, Characterization of stochastic resonance in a bistable system with Poisson white noise using statistical complexity measures, Commun. Nonlinear Sci. Numer. Simul. 28 (2015) 39–49.
[26] B. Godó, A. Nagy, Detecting regular and chaotic behaviour in the parameter space by generalised statistical complexity measures, Chaos Solitons Fractals 78 (2015) 26–32.
[27] X. Calbet, R. López-Ruiz, Tendency towards maximum complexity in a nonequilibrium isolated system, Phys. Rev. E 63 (2001) 066116.
[28] L. Zunino, M.C. Soriano, O.A. Rosso, Distinguishing chaotic and stochastic dynamics from time series by using a multiscale symbolic approach, Phys. Rev. E 86 (2012) 046210.
[29] P.M. Saco, L.C. Carpi, A. Figliola, E. Serrano, O.A. Rosso, Entropy analysis of the dynamics of el nino/southern oscillation during the holocene, Physica A 389 (2010) 5022–5027.
[30] C.E. Shannon, A mathematical theory of communication, Bell Syst. Tech. J. 27 (1948) 379–423. 623–656.
[31] P.W. Lamberti, M.T. Martín, A. Plastino, O.A. Rosso, Intensive entropic non-triviality measure, Physica A 334 (1) (2004) 119–131.
[32] R. López-Ruiz, H.L. Mancini, X. Calbet, A statistical measure of complexity, Phys. Lett. A 209 (5–6) (1995) 321–326.
[33] M. Zanin, L. Zunino, O.A. Rosso, D. Papo, Permutation entropy and its main biomedical and econophysics applications: a review, Entropy 14 (2012) 1553–1577.
[34] A.L.L. Aquino, T.S.G. Cavalcante, E.S. Almeida, A. Frery, O.A. Rosso, Characterization of vehicle behavior with information theory, Eur. Phys. J. B 8 (2012) 257.
[35] F. Montani, O.A. Rosso, F. Matias, S.L. Bressler, C.R. Mirasso, A symbolic information approach to determine anticipated and delayed synchronization in neuronal circuit models, Philos. Trans. R. Soc. Lond. Ser. A 373 (2015) 20150110.
[36] F. Montani, R. Baravalle, L. Montangie, O.A. Rosso, Causal information quantification of prominent dynamical features of biological neurons, Philos. Trans. R. Soc. Lond. Ser. A 373 (2015) 20150109.
[37] A. Bariviera, M.B. Guercio, L.B. Martinez, O.A. Rosso, A permutation information theory tour through different interest rate maturities: the Libor case, Philos. Trans. R. Soc. Lond. Ser. A 373 (2015) 20150119.
[38] A. Bariviera, M.B. Guercio, L.B. Martinez, O.A. Rosso, The (in)visible hand in the libor market: an information theory approach, Eur. Phys. J. B 88 (2015) 208.
[39] J. Kolter, S. Batra, A. Ng, Energy disaggregation via discriminative sparse coding, in: Neural Information Processing Systems, 2010, pp. 1–9.
[40] J. Kolter, T. Jaakkola, Approximate inference in additive factorial HMMs with application to energy disaggregation, J. Mach. Learn. Res.–Proc. Track (JMLR) 22 (2012) 1472–1482.
[41] M. Wytock, J.Z. Kolter, Contextually supervised source separation with application to energy disaggregation, in: AAAI Conference on Artificial Intelligence, 2014, pp. 486–492.
[42] H. Kim, M. Marwah, M. Arlitt, G. Lyon, J. Han, Unsupervised disaggregation of low frequency power measurements, in: SIAM Conference on Data Mining, 2011, pp. 747–758.
[43] H. Shao, M. Marwah, N. Ramakrishnan, A temporal motif mining approach to unsupervised energy disaggregation: Applications to residential and commercial buildings, in: AAAI Conference on Artificial Intelligence, 2013, pp. 1327–1333.